scientific reports

OPEN

A prospective cohort study develops and validates a machine learning model for predicting ecchymosis after total knee arthroplasty

Xuefeng Luo[1,2,5], Wei Bao[1,3,5], Yu Ye[4], Runxing Kang[1,2], Wei Xu[1,2✉], Wei Huang[1,2✉] & Junyi Liao[1,2✉]

Total knee arthroplasty (TKA) is a standard procedure for end-stage knee diseases, yet perioperative bleeding and its complications, such as ecchymosis, remain significant challenges. Predicting ecchymosis can guide personalized perioperative blood management, enhancing patient recovery and reducing the socioeconomic burden. In this prospective study (June 2023–March 2024), 416 TKA patients were split into ecchymosis (n = 135) and non-ecchymosis (n = 281) groups. The first seven months' data (312 patients) were used for training, and the next three months' (104 patients) for validation. Feature selection used Least Absolute Shrinkage and Selection Operator (LASSO), Random Forest-Recursive Feature Elimination (RF-RFE), and BORUTA to identify key risk factors. The model was tested with advanced machine learning: Random Forest (RF), eXtreme Gradient Boosting (XGBoost), Support Vector Machines (SVM), and Light Gradient Boosting Machine (LGBM). Major risk factors included low prealbumin, reduced coagulation index (CI) and its change (XCI), high fibrinogen degradation products (FDP), and postoperative day 1 total blood loss (TBL). The model showed robust performance with area under the curve values (AUCs) of 0.927 in training and 0.954 in validation set. The model's superior high performance offers significant guidance for early and accurate prediction, enabling personalized anticoagulation therapy and optimizing perioperative blood management in TKA patients.

Trial registration: Chinese Clinical Trial Registry (registration No. ChiCTR2400080173).

Abbreviations

TKA	total knee arthroplasty
POD	postoperative day
PAD	postadmission day
TBL	total blood loss
FDP	fibrinogen degradation products
CI	coagulation index
XCI	CI. POD1-CI. PAD
ML	machine learning

[1]Department of Orthopaedic Surgery, The First Affiliated Hospital of Chongqing Medical University, Chongqing 400016, China. [2]Chongqing Municipal Health Commission Key Laboratory of Musculoskeletal Regeneration and Translational Medicine, Orthopaedic Research Laboratory of Chongqing Medical University, Chongqing 400016, China. [3]Department of Orthopaedics, Banan Hospital of Chongqing Medical University, Chongqing 401320, China. [4]Department of Orthopaedics, The Second People's Hospital of Yubei District, Chongqing 401147, China. [5]Xuefeng Luo and Wei Bao contributed equally to this work. ✉email: 30545400@qq.com; huangwei68@263.net; liaojunyi@cqmu.edu.cn

nature portfolio

1

Lgbm	lightgbm
LM	logistic regression model
RF	random forest
SVM	support vector machine
Xgboost	extreme gradient boosting

Total knee arthroplasty (TKA) has been recognized as one of the most significant advancements in effectively treating end-stage knee diseases since the 20th century[1–3]. With the increasing number of TKA procedures, there is growing attention to perioperative anemia, blood loss and blood transfusion[4,5]. Therefore, effective perioperative blood management is essential for promoting recovery and reducing the social and economic burden in TKA patients[6,7].

Coagulation and bleeding are the two primary components of perioperative blood management, working synergistically to maintain hemostasis balance[8]. However, the prevention of bleeding risk remains a concern among orthopedic surgeons in patients receiving TKA[9–11]. Although regular adoption of anticoagulants has reduced the incidence of perioperative venous thromboembolism (VTE) to as low as 0.5%−1% in TKA patients[12]. However, postoperative blood loss is still posing considerable challenges to its effective management. Statistics reveal that perioperative blood loss in major orthopedic surgeries such as TKA could reach up to 1200 ml[13], with over 53.2% of patients developing moderate or severe hemorrhagic anemia[14]. Inadequate management of perioperative bleeding can result in a series of bleeding-related complications, including ecchymosis, systemic hemorrhage, and coagulation disorders, significantly compromising postoperative functional recovery and patient satisfaction[15,16]. Therefore, to better navigate this trade-off, there is an urgent need for surgeons that can accurately predict bleeding events in patients undergoing anticoagulation therapy.

As one of the most common signs of postoperative bleeding events, the incidence rate of postoperative ecchymosis is as high as 30–40%[15,17–19]. As subcutaneous bleeding exceeds 3 mm in diameter, ecchymosis often accompanies wound or severe swelling and pain in the lower limb, exacerbating local inflammation and signifying an increased tendency for further blood loss[20–22]. Meanwhile, post-operative ecchymosis generally indicates a hypocoagulable state[18]. Failure to promptly detect and intervene may significantly increase the risk of secondary bleeding, potentially leading to systemic coagulopathy, major hemorrhage, and even mortality[23,24]. Therefore, the prediction of post-operative ecchymosis can reserve the time window for personalized perioperative blood management strategies, decreasing the occurrence rates of postoperative anemia, blood loss and blood transfusion. Although several recent research explored the risk factors for postoperative ecchymosis[17,19,25], the integration of these factors remains incomplete and lacks prospective evidence, necessitating further improvements in predictive accuracy and effectiveness.

With the rapid development of Machine Learning (ML), its application in precise clinical diagnostics and treatments has gained increasing popularity[26–28]. Unlike traditional statistical methods, ML combines computer technology and artificial intelligence for data organization and mining, offering significant advantages in managing complex issues like over-fitting and non-linearity in big data, often resulting in higher predictive accuracy[29,30]. To leverage ML for developing a predictive model for postoperative bleeding, using postoperative ecchymosis as an indicator, we designed this prospective cohort study to collect perioperative data from patients undergoing TKA for model development. Meanwhile, various ML techniques are employed to validate this model and prospectively assess its accuracy. The predictive model offers a critical time window for personalized perioperative blood management strategies, enhancing rapid recovery for TKA patients.

Participants and methods
Participants
From June 2023 to March 2024, patients diagnosed with end-stage osteoarthritis and scheduled for TKA at our medical center were screened based on strict inclusion and exclusion criteria. Inclusion criteria included: (1) Patients who received unilateral primary TKA due to end-stage knee diseases. (2) Age ≥ 18 years. Exclusion criteria included: (1) Patients with severe cardiovascular and cerebrovascular diseases (myocardial infarction, cerebral infarction, etc.); (2) Patients with significant bleeding tendencies (such as gastrointestinal active bleeding, cerebral hemorrhage, etc.); (3) Patients with systemic or local venous thromboembolism (such as deep vein thrombosis, pulmonary embolism, etc.); (4) Patients with previously defined coagulation dysfunction; (5) Patients with severe neuromuscular system diseases; (6) Patients scheduled for bilateral TKA or revision TKA; (7) Pregnant or breastfeeding patients. To maintain the precision of the trial and minimize variation, all surgical procedures were performed by the same experienced surgical team.

Surgical procedure
Following patient selection based on defined inclusion and exclusion criteria, all TKA surgeries were consistently performed by the same experienced surgical team, which included two senior surgeons with more than 20 years of experience to ensure standardization. All procedures strictly followed a standardized perioperative management protocol that included aspects such as anesthesia, pain control, medication, rehabilitation, and nursing. To ensure data integrity, all patients underwent identical blood tests and examinations consistently before and after surgery.

Each patient was positioned in a supine posture with a pneumatic tourniquet applied to the thigh of the affected leg. The surgeries adhered to standardized TKA protocols, involving precise bone cutting and fitting a uniform type of knee joint prosthesis. Intraoperative X-ray imaging ensured accurate positioning of the prosthesis before the wound was methodically sutured. A local 1 g dose of tranexamic acid (TXA) was administered, and no postoperative drainage tubes were used. Furthermore, each patient received a 1.5 g intravenous dose of TXA every 12 h post-surgery to manage bleeding.

General perioperative management

Anesthesia Protocol: All patients underwent TKA surgery using the same anesthetic agents, which included midazolam and propofol for sedation, remifentanil for pain relief, and vecuronium for muscle relaxation.

Pain Management Protocol: Post-surgical pain management for all patients was managed with a patient-controlled intravenous analgesia pump containing 0.1 mg of sufentanil and 100 mg of flurbiprofen axetil.

Infection Prevention Medication: From postoperative Day 1 to Day 3 (POD1-POD3), all patients received 1.5 g of cefuroxime every 12 h to prevent infection.

Mechanical and Drug Prophylaxis for VTE: To prevent VTE, intermittent pneumatic compression was administered twice daily, with each session lasting 20 min. Meanwhile, each patient received a a once-daily postoperative subcutaneous injection of 4,000 IU of low-molecular-weight heparin.

Nursing Care Protocol: All enrolled patients were managed perioperatively by the same nursing team, receiving consistent intravenous fluid types and dosages, with meticulous monitoring and recording of input and output over 24 h.

Nutritional Management: On the morning of surgery, all patients consumed an equal dose of short peptides plus whole protein enteral nutrition. Their intake and output were rigorously monitored, and their nutritional status, including albumin and prealbumin levels, was closely observed before and after surgery.

Observation and grouping

All patients who underwent TKA surgery were closely monitored postoperatively for the occurrence of ecchymosis around the incision and thigh area and grouped accordingly. If ecchymosis with subcutaneous bleeding exceeding 3 mm in diameter was observed, its location and size were precisely documented, and the patient was categorized into the ecchymosis group. Patients without ecchymosis were classified into the non-ecchymosis group. All enrolled patients underwent the same blood tests and other relevant examinations pre-operatively and on POD1.

Blood loss calculation

The hidden blood loss (HBL) of every patient is calculated according to Nadler et al.[31] and Gross formula[32]:

1): Patient blood volume (PBV, mL) = [k1 × height^3 (m) + k2 × weight (kg) + k3] × 1000, where k1 = 0.3669, k2 = 0.03219, and k3 = 0.6041 for male, and k1 = 0.3561, k2 = 0.03308, and k3 = 0.1833 for female.

2): Total blood loss (TBL, mL) = PBV × (preoperative Hct - postoperative Hct)/preoperative Hct.

3): Intraoperative blood loss (IBL) = volume collected by suction - volume of irrigation + weight of blood-soaked gauze, where 1 g of gauze = 1 ml.

Feature selection

Fifty-six features, including patient demographics and surgical details such as age, gender, BMI, surgical duration, intraoperative blood loss, and TBL on both preoperative and POD1 were included. Routine hematology parameters included hemoglobin (Hb), hematocrit (HCT), platelet count (PLT), mean platelet volume (MPV), and platelet distribution width (PDW). Nutritional indicators included total protein, prealbumin, and albumin. The coagulation function indicators comprised prothrombin time (PT), activated partial thromboplastin time (APTT), thrombin time (TT), international normalized ratio (INR), fibrinogen, fibrinogen degradation products (FDP), and D-dimer. Thromboelastography (TEG) measured several critical parameters: reaction time (R), clot formation time (K), alpha angle (angle), maximum amplitude (MA), lysis at 30 min (LY30), and the coagulation index (CI), a composite measure of overall coagulation status derived from R, K, angle, and MA values[33]. Change in coagulation index was calculated as XCI = CI. POD1 - CI. PAD (postadmission day).

First, in the training set, univariate logistic regression was applied to screen for potential risk factors with a significance threshold of $P < 0.05$. This initial screening identified 15 candidate variables. Subsequently, to refine this list and select the most stable and important features, we employed three distinct machine learning-based algorithms on the training set: Least Absolute Shrinkage and Selection Operator (LASSO), the Boruta algorithm, and Random Forest-Recursive Feature Elimination (RF-RFE). The final set of key risk factors was determined by taking the intersection of the variables selected by all three of these methods.

Model development

All TKA patients were randomly assigned to the training and validation sets in a 7:3 temporal ratio at the onset of the study (first seven months for training, subsequent three months for validation). This temporal split was intentionally chosen over a random split to simulate a real-world clinical application scenario, where a model is built on historical data and validated on future patients. This approach provides a more rigorous assessment of the model's generalizability and robustness over time and helps prevent temporal data leakage. It is important to note that no variables, including sex, were explicitly matched, or stratified during this split. The distribution of all baseline characteristics was a result of the natural variation within these consecutively enrolled temporal cohorts.

LASSO regression was primarily utilized for feature selection. It identified essential features by modifying the optimization objective function with a penalty term to encourage sparsity, thereby reducing many feature weights to zero. Meanwhile, LASSO was used to exclude non-significant features, thus constructing sparse and interpretable models to prevent overfitting[34].

The Boruta algorithm was applied to evaluate feature importance with random forests and compare randomly generated "shadow" features, effectively addressing the challenges of feature selection[35].

RF-RFE was used to integrate the inherent feature selection capability of Random Forest into a recursive feature elimination strategy. By iteratively training the model and eliminating the least important features, RF-

RFE optimized feature subsets to enhance model performance, reduce computational overhead, and improve model interpretability[36].

After applying these three primary ML techniques to the training set data for essential variables filtering, the final variable results to identify critical risk factors were intersected. Using these risk factors, the predictive model was generated by multivariate logistic regression analysis and visualized by using line plots.

Model evaluation and validation

Several key statistical tools were utilized to comprehensively assess our predictive model. The Receiver Operating Characteristic (ROC) curve was employed to evaluate the model's ability to differentiate between two types of outcomes—whether or not ecchymosis occurred after TKA. Area Under the Curve (AUC) was applied to indicate diagnostic accuracy, reported with 95% confidence intervals (CI). Additionally, calibration curves were utilized to test the model's predictive accuracy. Decision Curve Analysis (DCA) was applied to balance patient benefits and risks while assessing the practicality of clinical decisions[37].

To benchmark the performance of our primary logistic regression model and validate the robustness of the selected features, we also constructed and evaluated four additional prediction models on the validation set using the same set of five key features. This selection was deliberate to encompass a range of model architectures and strengths: Random Forest (RF) was chosen for its robustness against overfitting, its ability to model complex non-linear relationships without strong assumptions about the data distribution, and its inherent provision of feature importance measures[38]. EXtreme Gradient Boosting (XGBoost) was selected due to its high predictive performance and efficiency in handling structured/tabular data. Its gradient-boosting framework is particularly effective at capturing intricate patterns through sequential model correction[39]. Support Vector Machines (SVM) were employed for their effectiveness in high-dimensional spaces and their ability to find a clear margin of separation (hyperplane) between classes, which is beneficial for binary classification tasks like ours[40]. Light Gradient Boosting Machine (LGBM) was utilized for its computational speed and memory efficiency, especially on large datasets, while maintaining high accuracy comparable to other boosting algorithms. For comparative purposes, a Logistic Regression (LM) model was also included as a well-understood and interpretable baseline, against which the performance of the more complex ML models could be benchmarked. The evaluation focused on the comparison of ROC curves, the analysis of feature importance distribution, and the assessment of SHAP values. Additionally, the performance metrics for each model—AUC, Accuracy, Sensitivity, Specificity, F1 Score, Recall, and Precision—were compared and summarized to validate the efficacy of the predictive model and identify the optimal ML approach.

Data analyses

Data processing was conducted using R software version 4.2.3 in this study. Missing values were addressed using Multiple Imputation by Chained Equations (MICE), and variables with more than 5% missing data were excluded from the analysis[41]. Descriptive analyses were performed on all patients included in the study. Continuous variables following a normal distribution were represented by mean ± standard deviation (SD) and analyzed using the t-test. For non-normally distributed continuous variables, the median (interquartile range) [M (P25, P75)] was used, with group comparisons conducted via the Mann-Whitney U test. Categorical variables were presented as n (%) and analyzed using the chi-square test, with Fisher's exact test applied when chi-square conditions were not met. All statistical tests were two-sided, and a P-value of < 0.05 was considered statistically significant. Multiple ML methods were implemented in R with packages in the supplementary materials.

Ethical considerations

This prospective cohort study was conducted in accordance with the CONSORT standards[42]. Ethical approval was granted by the local Ethics Committee, and the study was registered with the Chinese Clinical Trial Registry (registration No. ChiCTR2400080173) before participants were enrolled. All eligible patients were fully informed of the benefits and risks associated with the study before signing the informed consent form to participate. All methods were done in accordance with relevant guidelines. They were also advised that they could withdraw from the study at any point if they experienced any discomfort.

Results

Baseline data

From June 2023 to March 2024, 468 patients undergoing TKA were included. After excluding 52 patients according to the inclusion and exclusion criteria, 416 were prospectively analyzed in this study (Fig. 1). Among these patients, 135 developed ecchymosis after TKA, constituting 32.5% of the total cohort. Ecchymosis of varying degrees and sizes was observed in areas such as the popliteal fossa, groin, lateral thigh, and around the surgical wound (Fig. 2A and F). We found that patients with post-TKA ecchymosis had significantly lower American Knee Society (AKS) scores compared to those without ecchymosis ($P < 0.001$, Fig. 2G), significantly higher TBL on POD1 ($P < 0.001$, Fig. 2H), and a significantly lower CI ($P < 0.001$, Fig. 2I). These findings indicate a hypocoagulable state and a higher risk of postoperative bleeding in patients with post-TKA ecchymosis. Consequently, constructing a post-TKA ecchymosis predictive model is necessary.

The construction of the predictive model was based on the training and validation sets. According to the admission dates, data from 312 patients (non-ecchymosis group: 205, ecchymosis group: 107) from June to December 2023 were assigned to the training set, while data from 104 patients (non-ecchymosis group: 76, ecchymosis group: 28) from January to March 2024 were allocated to the validation set (Fig. 1). Baseline data for patients in the training and validation sets are presented in Table 1, while complete baseline data for all participants are available in **Table S1**. The rationale for the division into training and validation sets is detailed in **Table S2**.
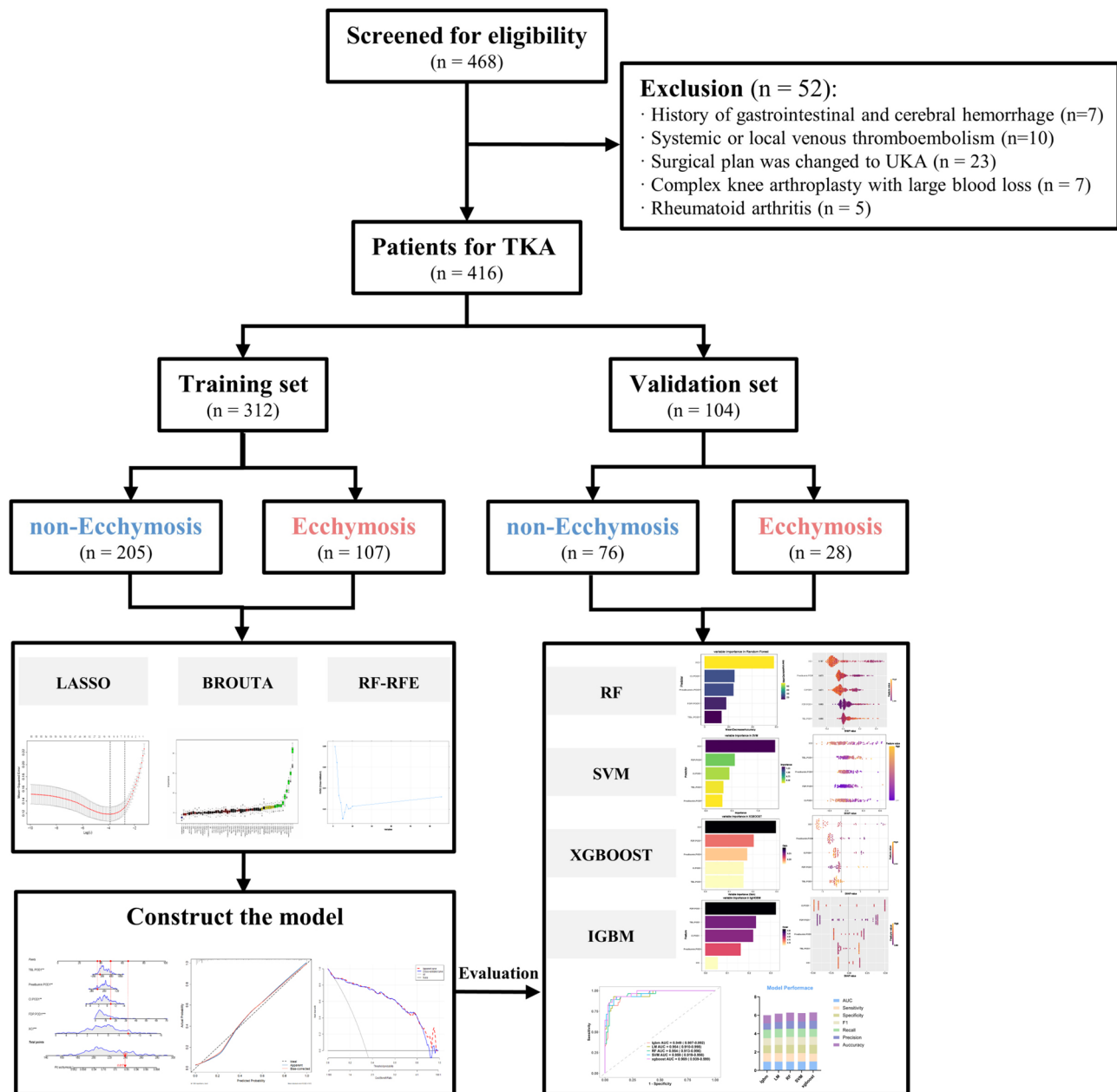
Fig. 1. The flowchart of this study. TKA, total knee arthroplasty. UKA, unicompartmental knee arthroplasty. RF, random forest. SVM, support vector machine. Xgboost, extreme gradient boosting. Lgbm, lightgbm.

Feature selection

Based on the training set, 15 potential risk factors were initially identified using univariate logistic regression with a significance threshold of $P < 0.05$; details can be found in Table 2 and **Figure S1**. The results of variable filtering and feature importance selection, using three ML algorithms (LASSO, BORUTA, RF-RFE), are displayed in Fig. 3. The results of all three methods were consistent, identifying five key factors: lower prealbumin ($P = 0.006$), CI ($P = 0.002$), XCI ($P < 0.001$), elevated levels of FDP ($P < 0.001$), and TBL ($P = 0.009$) on POD1, detailed in Table 3.

Construction of prediction model

Three ML algorithms, including LASSO, BORUTA, and RF-RFE, were applied to verify the five key variables essential for constructing the predictive model. The model's coefficients were visualized in a nomogram (Fig. 4A), which allows clinicians to input a patient's clinical data and rapidly compute the probability of postoperative ecchymosis in TKA patients. The formula for predicting ecchymosis probability is as follows: Ecchymosis prediction probability $= 1.186066 - 0.017569 \times$ Prealbumin. POD1 $+ 0.002506 \times$ TBL. POD1 $- 0.463744 \times$ CI. POD1 $- 1.163408 \times$ XCI $+ 0.112593 \times$ FDP. POD1. Meanwhile, the prediction model has been developed into a dynamic nomogram and registered on the website, allowing for real-time online prediction of the probability
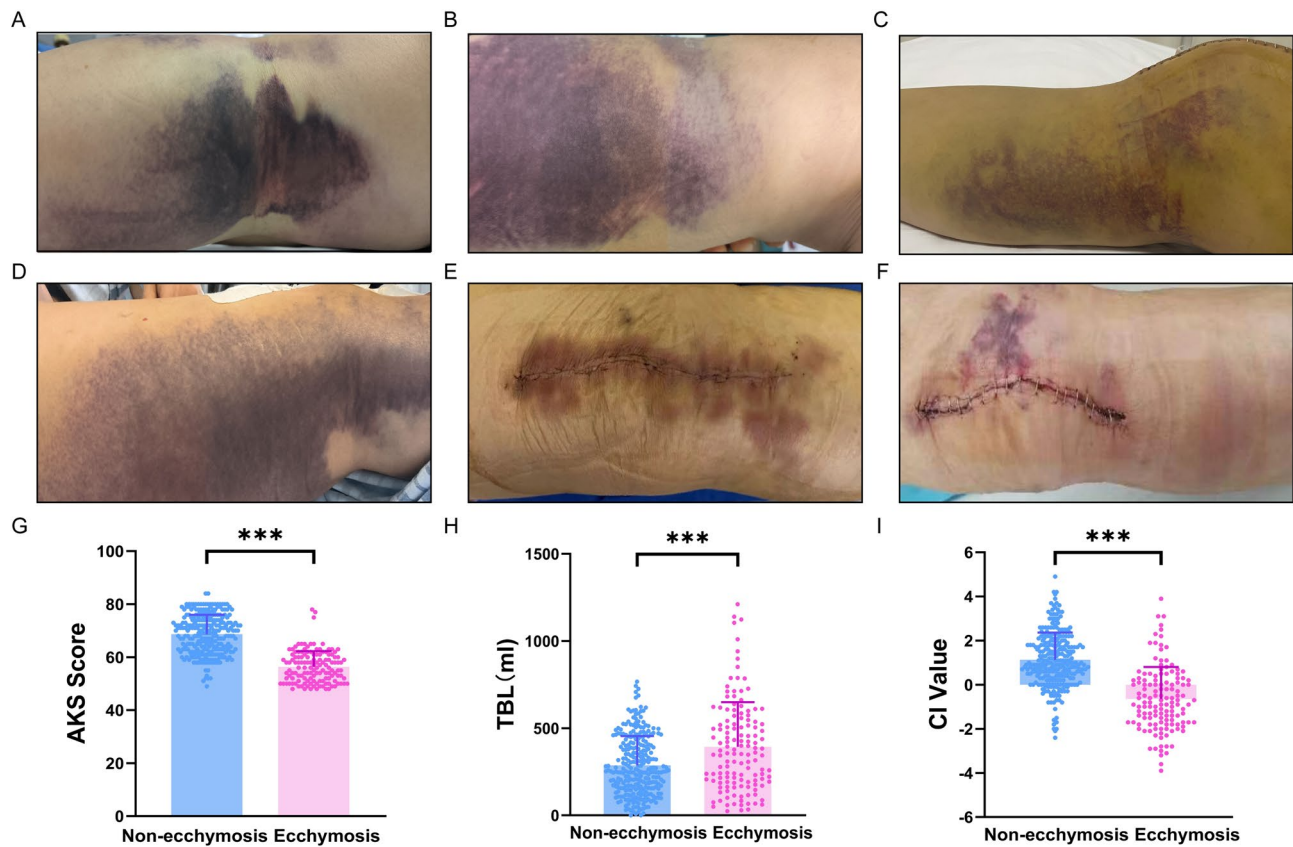
Fig. 2. Appearance of ecchymosis on different body parts and their different scores compared to non-ecchymosis population. (**A-F**): Ecchymosis of varying degrees and sizes appeared in different areas. (**A**): Popliteal ecchymosis. (**B**): Ecchymosis at the base of the thigh. (**C**): Ecchymosis on the calf. (**D**): Ecchymosis on the lateral thigh. (**E**): Ecchymosis at the wound site. F: Ecchymosis adjacent to the wound. (**G**): Lower AKS scores in ecchymosis patients. (**H**): Higher TBL in ecchymosis patients. (**I**): Lower CI values in ecchymosis patients. AKS, American Knee Society. TBL, total blood loss. CI, coagulation index. ***, $P < 0.001$.

of bruising post-TKA surgery (Fig. 4B). The specific information about the online version of the prediction model can be found in **Figures S2 & S3**. Subsequently, the five variables from the training and validation sets were compared with our nomogram (Fig. 4C and D). The ROC curves clearly demonstrate that the nomogram's AUC values are superior to those of individual variables, thereby validating the effectiveness of our prediction model. Finally, to internally validate the model's discriminatory power and consistency, we applied the model's formula to calculate the ecchymosis probability for every patient in both the training and validation sets. The results demonstrated that the model-assigned probability scores were significantly higher for patients in the observed ecchymosis group compared to those in the non-ecchymosis group (Fig. 4E and F). This consistent pattern across both datasets confirms that the model's predictions are well-calibrated and reliably separate the two outcome groups, thereby underscoring its repeatability and clinical utility.

Evaluation of the prediction model

The initial validation of our predictive model demonstrated robust performance. The AUC for the training cohort was 0.927 (95% CI, 0.891-0.891 0.962) (Fig. 5A), while the AUC for the validation cohort reached 0.954 (95% CI, 0.910–0.998) (Fig. 5B). Calibration plots and Hosmer-Lemeshow tests ($P > 0.05$) indicated good consistency between the predicted probabilities of post-TKA ecchymosis and the observed probabilities in both the training and validation sets (Fig. 5C and D). In the clinical application of our nomogram, Decision Curve Analysis (DCA) was conducted, revealing that the nomogram provided greater net benefits than other models (Fig. 5E and F). This evidence confirmed the model's accuracy and clinical utility in predicting the risk of ecchymosis post-TKA.

Model validation based on multiple ML algorithms

The predictive performance of the five key features was further substantiated by building four independent prediction models on the validation set using different ML algorithms. RF, SVM, XGBoost, and LGBM models were used to reassess feature importance, draw ROC curves, and create SHAP value plots. These analyses consistently confirmed the strong predictive capability of the model (Fig. 6).

Characteristic	Training set (n = 312)			Validation set (n = 104)		
	Non-ecchymosis (n = 205)	ecchymosis (n = 107)	P	Non-ecchymosis (n = 76)	ecchymosis (n = 28)	P
Sex:			1.000			1.000
Women (%)	181 (88.29)	95 (88.79)		67 (88.16)	25 (89.29)	
Men (%)	24 (11.71)	12 (11.21)		9 (11.84)	3 (10.71)	
Age	69.00 [66.00;72.00]	70.00 [66.50;75.50]	0.049	69.00 [64.00;73.00]	69.00 [66.25;70.25]	0.921
Prealbumin.POD1	206.60 (28.11)	182.68 (32.61)	<0.001	203.50 [194.50;226.25]	170.00 [158.00;209.50]	<0.001
TBL.POD1	246.16 [143.55;393.01]	347.92 [199.33;505.69]	<0.001	312.81 [193.25;442.40]	429.29 [150.05;729.86]	0.035
Hct.PAD	38.39 (3.40)	39.18 (3.81)	0.071	38.80 [36.38;41.30]	39.25 [37.48;40.65]	0.698
Hct.POD1	35.52 (3.33)	35.11 (3.27)	0.300	35.58 (3.57)	33.86 (4.72)	0.089
CI.POD1	1.17 (1.24)	−0.49 (1.51)	<0.001	1.04 (1.18)	−1.22 (0.95)	<0.001
XCI	1.02 (1.13)	−0.93 (1.45)	<0.001	1.16 (1.31)	−1.42 (1.28)	<0.001
FDP.POD1	5.60 [3.30;10.10]	9.40 [5.90;16.15]	<0.001	6.20 [3.98;8.93]	10.10 [5.50;18.12]	0.016
BMI	26.00 [23.40;28.10]	25.60 [23.45;27.40]	0.324	26.00 [23.40;28.30]	26.20 [23.92;28.13]	0.939
Operation time	85.00 [75.00;100.00]	85.00 [75.00;100.00]	0.761	85.00 [70.00;100.00]	90.00 [72.50;100.00]	0.672
IBL	44.00 [34.00;50.00]	41.00 [37.50;50.00]	0.268	50.00 [35.50;50.00]	42.00 [38.00;47.25]	0.250
Prealbumin.PAD	220.00 [198.00;242.00]	213.00 [189.00;232.50]	0.049	227.00 [207.25;243.75]	208.50 [182.00;241.00]	0.033
Totalalbumin.PAD	67.00 [65.00;71.00]	68.00 [63.50;72.00]	0.996	67.78 (4.82)	68.68 (4.34)	0.366
Albumin.PAD	42.00 [41.00;44.00]	42.00 [40.00;44.00]	0.562	42.00 [41.00;43.00]	42.00 [41.00;43.00]	0.571
Albumin.POD1	38.00 [37.00;40.00]	38.00 [36.00;39.00]	0.012	38.00 [37.00;40.00]	36.50 [34.75;38.00]	0.002
Totalalbumin.POD1	62.00 [59.00;66.00]	61.00 [57.00;64.00]	0.004	61.54 (4.13)	59.89 (5.18)	0.138
Hb.PAD	125.78 (11.85)	127.06 (14.05)	0.422	126.50 [117.00;135.00]	125.00 [121.75;133.00]	0.814
Hb.POD1	115.74 (11.57)	113.65 (12.06)	0.144	115.21 (12.60)	109.71 (15.08)	0.093
PBV	3605.36 [3361.48;4002.32]	3575.46 [3277.74;3997.83]	0.342	3683.33 [3375.14;4036.88]	3460.11 [3183.22;3968.08]	0.192
TBL.POD3	552.58 [362.41;748.35]	592.80 [417.09;858.15]	0.061	593.93 (279.22)	727.54 (374.23)	0.093
PLT.PAD	201.00 [172.00;233.00]	203.00 [178.00;245.00]	0.555	205.89 (62.62)	207.14 (54.53)	0.921
PDW.PAD	13.60 [11.90;15.60]	13.40 [11.80;15.40]	0.685	12.95 [11.78;15.22]	13.00 [11.47;14.72]	0.657
MPV.PAD	11.10 [10.40;11.80]	11.10 [10.40;11.85]	0.949	10.80 [10.47;11.43]	10.95 [10.43;11.45]	0.840
PLT.POD1	192.00 [162.00;224.00]	194.00 [162.00;221.50]	0.909	191.20 (50.80)	187.89 (49.16)	0.764
PDW.POD1	13.80 [12.00;15.50]	13.10 [11.85;15.00]	0.360	13.05 [11.78;14.50]	14.00 [12.42;14.85]	0.344
MPV.POD1	11.22 (1.12)	11.23 (1.09)	0.960	10.90 [10.40;11.70]	11.15 [10.67;11.72]	0.179
FDP.PAD	1.30 [0.90;2.90]	1.50 [1.00;2.70]	0.525	1.35 [0.80;3.20]	1.45 [0.80;2.90]	0.962
DD.PAD	0.50 [0.30;1.03]	0.60 [0.40;1.10]	0.183	0.49 [0.30;1.06]	0.52 [0.30;1.65]	0.744
DD.POD1	3.19 [1.84;6.80]	4.50 [2.56;8.20]	0.002	2.92 [1.87;6.58]	4.95 [2.10;7.95]	0.113
PT.PAD	12.70 [12.40;13.20]	13.00 [12.60;13.20]	0.004	12.80 [12.40;13.00]	12.95 [12.38;13.50]	0.284
PTR.PAD	1.00 [0.95;1.00]	1.00 [0.97;1.00]	0.091	1.00 [0.95;1.00]	1.00 [0.92;1.00]	0.871
INR.PAD	0.98 [0.91;1.00]	1.00 [0.94;1.00]	0.007	0.99 [0.93;1.00]	1.00 [0.90;1.00]	0.832
PTA.PAD	107.00 [98.00;114.00]	104.00 [99.50;111.00]	0.499	106.00 [98.00;113.00]	103.00 [96.50;115.75]	0.679
APTT.PAD	34.50 [31.90;36.20]	34.40 [32.30;36.60]	0.463	33.10 [31.70;35.82]	34.45 [31.80;38.02]	0.253
TT.PAD	17.50 [16.60;18.40]	17.40 [16.70;18.10]	0.393	17.55 [16.70;18.30]	17.55 [16.82;18.60]	0.663
Fgb.PAD	3.26 [2.90;3.80]	3.03 [2.70;3.67]	0.012	3.20 [2.74;3.63]	2.92 [2.68;3.42]	0.205
PT.POD1	13.30 [12.90;13.70]	13.60 [12.90;14.10]	0.131	13.20 [12.80;13.70]	13.40 [12.95;14.22]	0.166
PTR.POD1	1.00 [0.99;1.04]	1.00 [1.00;1.10]	0.222	1.00 [0.99;1.03]	1.00 [1.00;1.10]	0.078
INR.POD1	1.00 [0.98;1.06]	1.00 [1.00;1.10]	0.137	1.00 [0.99;1.06]	1.02 [1.00;1.10]	0.102
PTA.POD1	98.00 [92.00;105.00]	95.00 [88.50;106.00]	0.212	98.50 [91.00;106.25]	95.00 [85.75;103.25]	0.117
APTT.POD1	32.90 [30.80;35.10]	33.60 [31.55;35.40]	0.203	32.90 [30.22;35.25]	32.95 [30.08;36.72]	0.578
TT. POD1	17.40 [16.40;18.20]	17.00 [16.20;18.30]	0.165	17.20 [16.30;18.20]	17.10 [16.08;18.22]	0.852
Fgb.POD1	3.17 [2.67;3.51]	3.10 [2.70;3.55]	0.919	3.12 [2.80;3.62]	2.82 [2.48;3.20]	0.020
R.PAD	6.40 [6.00;7.00]	6.40 [5.65;6.80]	0.512	6.40 [6.00;6.90]	6.40 [5.20;7.55]	0.865
K.PAD	1.50 [1.30;1.70]	1.50 [1.30;1.80]	0.772	1.50 [1.48;1.80]	1.50 [1.30;1.72]	0.258
Angle.PAD	67.40 [64.80;69.40]	67.40 [62.85;69.75]	0.815	67.40 [64.05;67.80]	67.60 [64.00;69.88]	0.307
MA.PAD	63.80 [61.60;66.20]	63.80 [61.00;66.55]	0.643	63.80 [62.38;65.08]	63.80 [60.43;65.40]	0.457
EPL.PAD	0.40 [0.00;1.00]	0.40 [0.00;0.80]	0.351	0.40 [0.00;0.62]	0.40 [0.00;1.00]	0.695
LY30.PAD	0.40 [0.00;1.00]	0.40 [0.00;0.80]	0.332	0.40 [0.00;0.60]	0.40 [0.00;0.88]	0.675
CI.PAD	0.00 [−0.40;1.00]	0.40 [−0.30;1.60]	0.058	0.00 [−0.72;0.90]	0.30 [−0.90;1.20]	0.411
R.POD1	5.91 (1.09)	6.42 (1.41)	0.001	6.00 [5.20;6.43]	6.80 [5.97;7.62]	<0.001
K.POD1	1.30 [1.20;1.60]	1.40 [1.20;1.80]	0.001	1.30 [1.20;1.40]	1.75 [1.37;2.20]	<0.001
Continued						

Characteristic	Training set (n = 312)		P	Validation set (n = 104)		P
	Non-ecchymosis (n = 205)	ecchymosis (n = 107)		Non-ecchymosis (n = 76)	ecchymosis (n = 28)	
Angle.POD1	69.00 [66.40;71.70]	67.50 [63.15;70.50]	0.001	68.65 [67.50;71.23]	62.90 [57.25;68.55]	<0.001
EPL.POD1	0.40 [0.00;1.10]	0.70 [0.10;1.65]	0.029	0.50 [0.00;1.22]	0.70 [0.30;1.40]	0.236
LY30.POD1	0.40 [0.00;1.10]	0.60 [0.10;1.65]	0.027	0.50 [0.00;1.20]	0.65 [0.30;1.18]	0.386

Table 1. Comparison results of general clinical characteristics on training set and validation set. Abbreviations: POD, postoperative day. PAD, PAD, postadmission day. Angle, alpha angle. K, clot formation time. R, reaction time. APTT, activated partial thromboplastin time. INR, international normalized ratio. PT, prothrombin time. TBL, total blood loss. FDP, fibrinogen degradation products. CI, coagulation index. XCI, CI. POD1-CI. PAD. BMI, Body Mass Index. IBL, intraoperative blood loss.

Characteristics	B	SE	OR	CI	Z	P
Angle. POD1	−0.093	0.02522	0.911	0.911(0.866–0.957)	−3.675	<0.001
K. POD1	1.241	0.32517	3.46	3.46(1.851–6.656)	3.818	<0.001
R. POD1	0.347	0.10296	1.415	1.415(1.162–1.742)	3.375	0.001
APTT.PAD	0.045	0.02205	1.046	1.046(1.007–1.099)	2.06	0.039
INR.PAD	2.803	1.31209	16.497	16.49(1.668–300.3)	2.136	0.033
PT.PAD	0.342	0.14813	1.408	1.408(1.113–1.965)	2.308	0.021
TBL.POD3	0.001	0.00039	1.001	1.001(1–1.002.002)	2.563	0.01
Totalalbumin.POD1	−0.086	0.02771	0.918	0.918(0.868–0.968)	−3.088	0.002
Albumin.POD1	−0.12	0.0447	0.887	0.887(0.811–0.967)	−2.675	0.007
FDP.POD1	0.099	0.01976	1.104	1.104(1.064–1.149)	5.002	<0.001
XCI	−1.453	0.17526	0.234	0.234(0.162–0.322)	−8.29	<0.001
CI.POD1	−0.91	0.11725	0.402	0.402(0.316–0.5.316.5)	−7.765	<0.001
TBL.POD1	0.003	0.00063	1.003	1.003(1.001–1.004)	4.173	<0.001
Prealbumin.POD1	−0.028	0.00478	0.972	0.972(0.963–0.981)	−5.919	<0.001
Age	0.039	0.01797	1.039	1.039(1.004–1.078)	2.144	0.032

Table 2. Single factor logistic regression analysis in training set. **Abbreviations**: POD, postoperative day. PAD, PAD, postadmission day. Angle, alpha angle. K, clot formation time. R, reaction time. APTT, activated partial thromboplastin time. INR, international normalized ratio. PT, prothrombin time. TBL, total blood loss. FDP, fibrinogen degradation products. CI, coagulation index. XCI, CI. POD1-CI. PAD.

Among the different ML methods, all demonstrated AUC values exceeded 0.9, indicating excellent model performance. Specifically, the AUC scores were as follows: LGBM: 0.949 (95% CI, 0.907–0.992); LM: 0.954 (95% CI, 0.910–0.998); RF: 0.954 (95% CI, 0.913–0.996); SVM: 0.959 (95% CI, 0.919–0.998); XGBoost: = 0.969 (95% CI, 0.939–0.999). Details comparing the effectiveness of each ML method were shown in Table 4; Fig. 6. In summary, the predictive model achieved satisfactory results across various ML validations, demonstrating its robustness and effectiveness in clinical settings.

Discussion

Osteoarthritis is one of the most debilitating diseases worldwide, and TKA remains one of the most effective treatments for end-stage osteoarthritis[43]. Recently, researchers have long been exploring and experimenting with bleeding and coagulation management after TKA. It is well-known that maintaining a delicate balance between coagulation and bleeding is challenging. Hence, personalized perioperative blood management was implemented to decrease blood loss without increasing the risk of VTE[10,12,17,44,45]. As a representative clinical sign of minor bleeding, newly formed ecchymosis also indicates a hypocoagulable state and should be paid attention to when establishing blood management schemes[15,18,45]. In the present study, taking ecchymosis as the "barometer" of postoperative bleeding, we constructed a post-TKA-ecchymosis predictive model using ML procedures, which would be applied to predicting postoperative bleeding and devising postoperative anticoagulation and hemostasis therapeutic strategies.

The clinical significance of predicting ecchymosis extends beyond its appearance. As our results showed, patients with ecchymosis had significantly lower early postoperative AKS scores (Fig. 2G). This suggests that ecchymosis, often accompanied by swelling and pain, can directly impede early functional recovery by discouraging active participation in physical therapy and limiting joint mobilization. Furthermore, extensive ecchymosis can cause significant patient anxiety and dissatisfaction, potentially affecting the overall perception of surgical success. Therefore, the ability to predict ecchymosis is not merely about anticipating a cosmetic issue, but about proactively managing a factor that can compromise early rehabilitation and patient-reported outcomes.
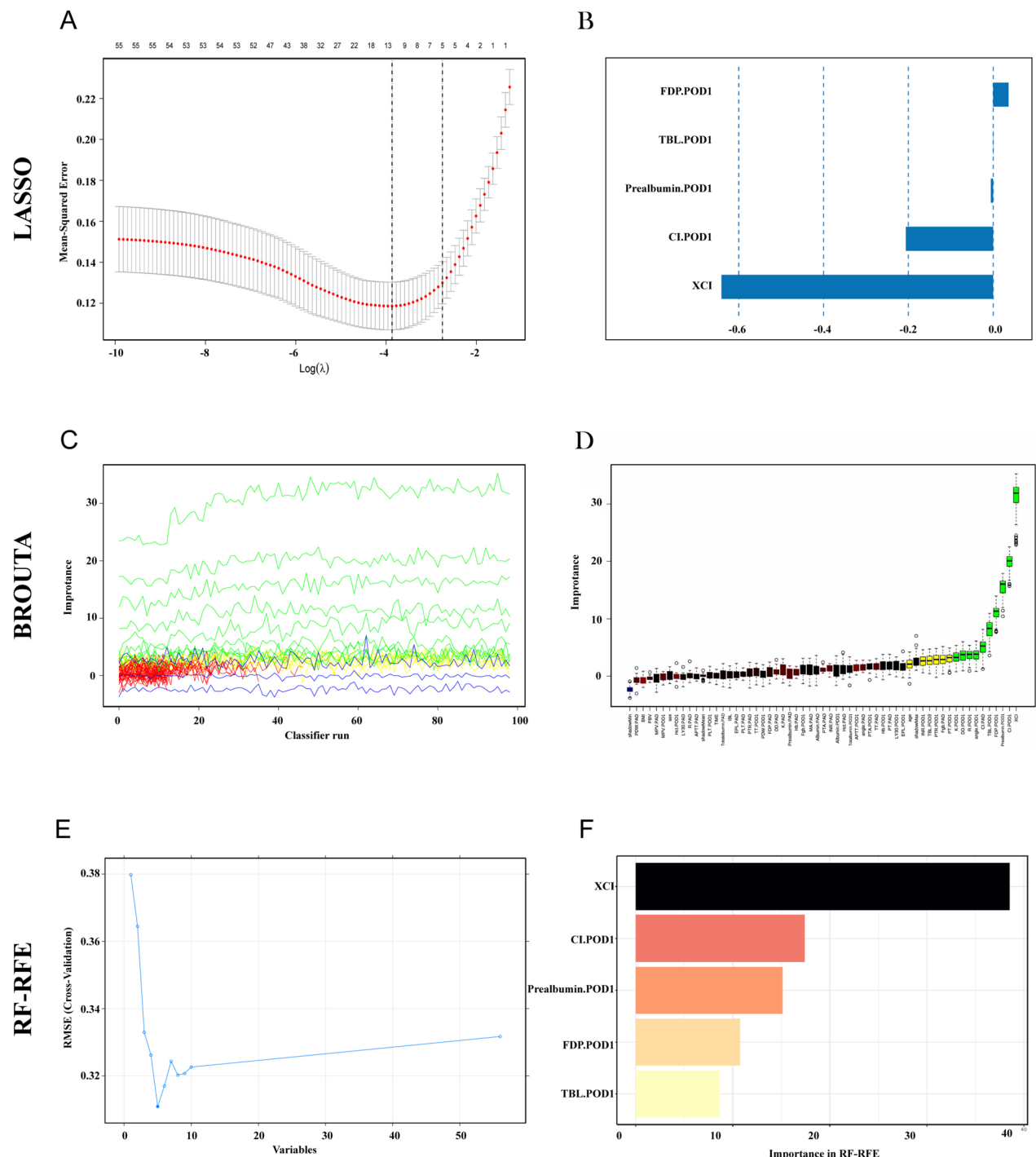
Fig. 3. Three machine learning methods for variable selection. (A&B): Log (λ) value and the five variables selected by LASSO. (C&D): The results selected using the Boruta. (E&F): The RF-RFE selected five variables with the minimum error, and the final distribution of variable importance.

Postoperative anemia is still one of the most common complications following TKA[44,46]. Increased hidden blood loss is a primary cause of postoperative anemia; therefore, balancing coagulation and bleeding is essential to decrease postoperative blood loss. Clinically, anticoagulation therapy in the early postoperative period remains controversial for ecchymosis patients, as it undoubtedly increases the risk of bleeding-related complications[15]. In a study from Germany, 42.9% of patients experienced bleeding complications after using anticoagulants, with 6.1% suffering from major bleeding, posing significant challenges for clinicians[47]. Similarly, for patients prone to bleeding, such as those with ecchymosis, anticoagulation raises the risk of developing bleeding, while discontinuing it in the short term raises concerns about an increased risk of thrombosis. Therefore, earlier and

Characteristics	B	SE	OR	CI	Z	P
(Intercept)	1.186	1.38029	3.274	3.274 (0.223–51.81)	0.859	0.39
Prealbumin.POD1	−0.018	0.00643	0.983	0.982 (0.969–0.994)	−2.734	0.006
TBL.POD1	0.003	0.00095	1.003	1.002 (1.000–1.004.000.004)	2.628	0.009
CI.POD1	−0.464	0.15194	0.629	0.628 (0.461–0.839)	−3.052	0.002
XCI	−1.163	0.2083	0.312	0.312 (0.201–0.457)	−5.585	< 0.001
FDP.POD1	0.113	0.028	1.119	1.119 (1.061–1.185)	4.022	< 0.001

Table 3. Multiple logistic regression analysis in training set. **Abbreviations**: POD, postoperative day. TBL, total blood loss. FDP, fibrinogen degradation products. CI, coagulation index. XCI, CI.POD1-CI.PAD.

accurate prediction of ecchymosis and intervention in risk factors can significantly benefit postoperative blood management and maintain the balance between coagulation and bleeding.

The rapid development of artificial intelligence has promoted advancements across various industries. Machine learning (ML), a branch of artificial intelligence, excels at managing, processing, and analyzing multidimensional data from large datasets efficiently and accurately, which can be beneficial in in clinical practice[48]. Unlike traditional statistical methods, ML adeptly identifies complex, multidimensional, and nonlinear relationships between clinical features in larger datasets, enhancing predictive performance. Consequently, it has achieved considerable success across various medical fields[49].

In the field of perioperative blood management after orthopedic surgery, abundant scoring systems and scales have been developed to assess the risk of VTE[50–52]. However, predictive models that can anticipate and manage bleeding tendencies remain rare. To address this gap, this prospective observational cohort study was designed to predict postoperative ecchymosis in patients undergoing TKA. The study precisely monitors, and groups patients based on the presence of ecchymosis around the surgical wound and thigh, ensuring accurate data collection. Furthermore, the data were divided into a training set and a validation set in a 7:3 ratio based on chronological order. This setup enables us to build the predictive model using the training set and subsequently conducted a temporal validation using the held-out future cohort. This setup allows us to evaluate the model's performance in a manner that closely mimics a prospective clinical application, thereby guaranteeing a realistic estimate of the model's accuracy upon deployment.

In selecting features of the predictive model, a comprehensive range of perioperative indicators were included, encompassing patient demographics, surgical details, nutritional status, coagulation profiles, TEG data, etc. Three sophisticated variable selection techniques — LASSO, RF-RFE, and BORUTA—were employed and identified five critical risk factors, enhancing the reliability and persuasiveness of the predictive model. To further validate the predictive model, multiple ML algorithms were employed, achieving strong results across key performance metrics such as AUC, sensitivity, specificity, F1 score, and recall. These outcomes not only validate the accuracy and feasibility of our predictive model but also highlight its potential applicability in clinical decisions.

Ecchymosis is regarded as a manifestation of subcutaneous hematoma, with current studies confirming that increased perioperative blood loss is linked to a higher likelihood of ecchymosis[15,17]. Correspondingly, postoperative ecchymosis could serve as a window of systemic coagulation status, as evidenced by authoritative research[18]. CI, a parameter in TEG that reflects the overall systemic coagulation index, is more sensitive than traditional coagulation profiles and is widely used[33]. A lower CI typically indicates a tendency for bleeding, which aligns with our findings. Moreover, our findings suggest that the higher XCI from preoperative to postoperative is also a risk factor for postoperative ecchymosis. This could be attributed to XCI's capacity to objectively reflect changes in coagulation states, thus influencing perioperative blood loss. Additionally, as a nutritional marker closely related to nutritional reserves and liver function, reduced prealbumin levels were observed to occur more frequently in patients with ecchymosis. It has been reported that insufficient nutrient reserves can impair the synthetic function of liver cells, directly leading to lowered levels of prealbumin and coagulation function[53,54]. Overall, the nutritional status of patients offers new insights into the treatment and management of ecchymosis. Blood clot formation and fibrinolysis are two complementary actions of coagulation[55]. Maintaining a balance between fibrinolysis and coagulation is crucial for hemostasis without excessive thrombosis risk. Excessively high-level activation of fibrinolysis generally indicates a bleeding tendency[56]. In the present study, we found that patients with ecchymosis exhibited higher levels of FDP on POD1, indicating heightened fibrinolysis. Certainly, these results further validate the rationale of our model, as its ROC values exceed those of each individual risk factor (Fig. 4C and D), consistently demonstrated across both the training and validation sets.

Regarding the natural history of this condition, postoperative ecchymosis typically follows a self-limiting course. Based on clinical observation and previous reports, the visible bruising often begins to fade within 1–2 weeks and usually resolves completely within 2–4 weeks, following the natural process of hemoglobin breakdown and reabsorption. However, the impact of its initial presence on the critical early recovery phase remains a concern. While our model effectively identifies patients at risk, the critical next step is to investigate how this early postoperative event influences long-term functional outcomes and overall prognosis after TKA. Future prospective studies with longer follow-up periods are essential to determine if ecchymosis is an independent risk factor for slower recovery, reduced range of motion, or lower patient satisfaction scores at 6 or 12 months. Such research would definitively establish the full clinical importance of our predictive model and guide the development of targeted interventions for high-risk patients.

This study has some limitations. Firstly, as a single-center study, there is potential bias in patient selection, and external validation with data from other medical institutions could strengthen our predictive model's
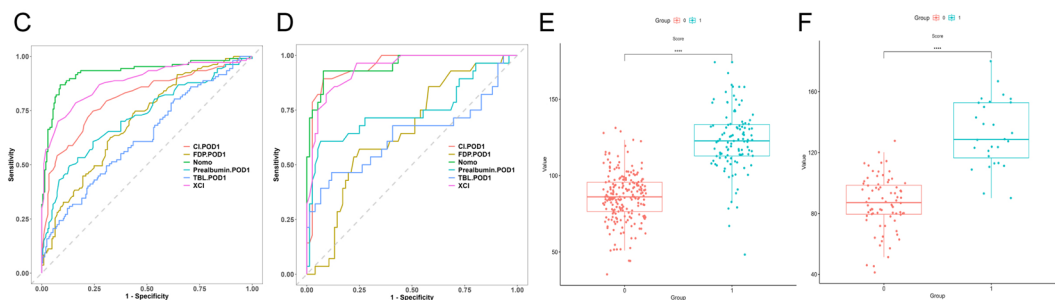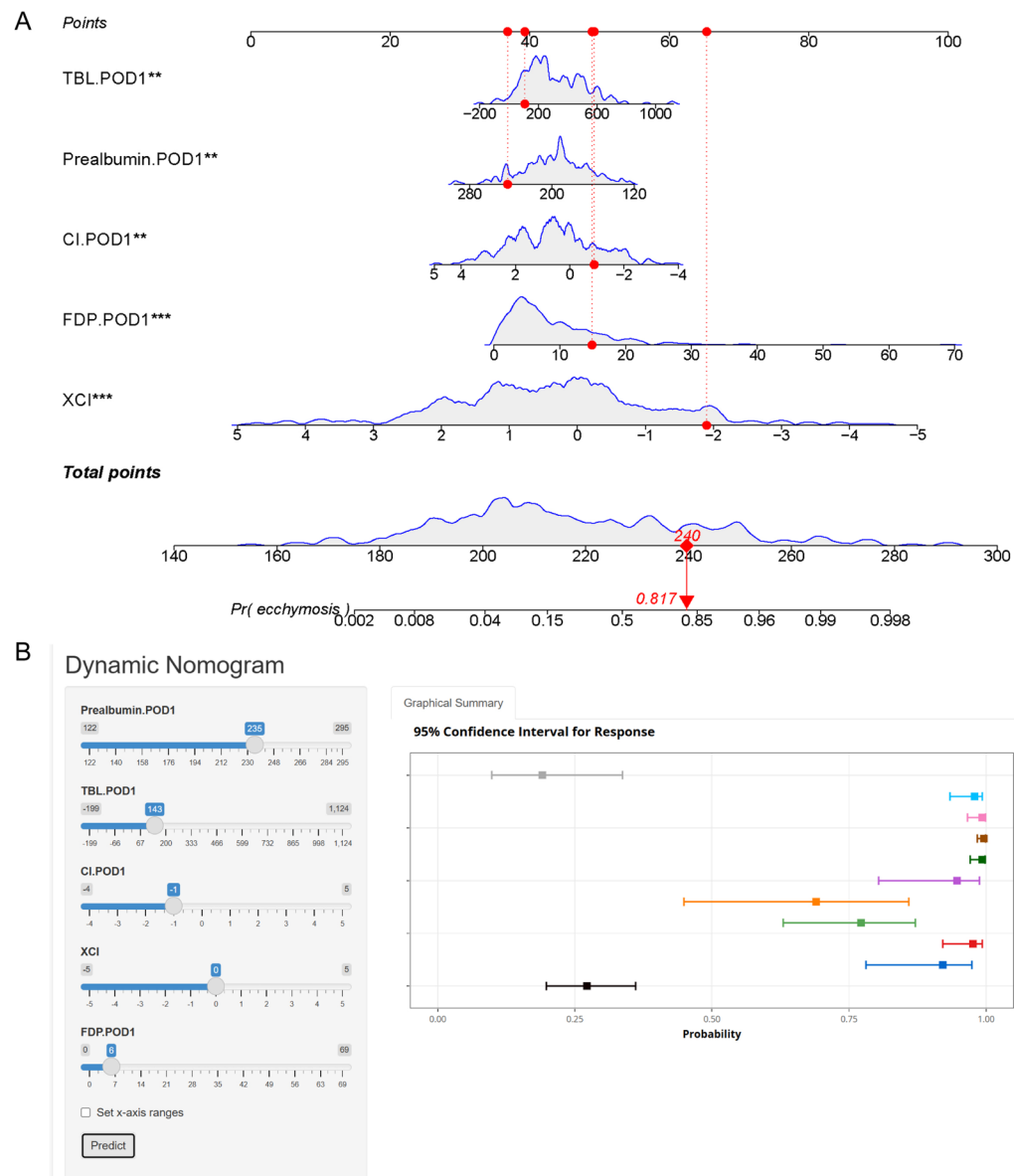
Fig. 4. Construction of the nomogram. (**A**): The nomogram for predicting ecchymosis. (**B**): The registration on the website for the dynamic nomogram. (**C**): The ROC curves of the nomogram and other variables in the training set. (**D**): The ROC curves of the nomogram and other variables in the validation set. (**E**): The nomoscore between non-ecchymosis group and ecchymosis group in the training set. (**F**): The nomoscore between non-ecchymosis group and ecchymosis group in the validation set.
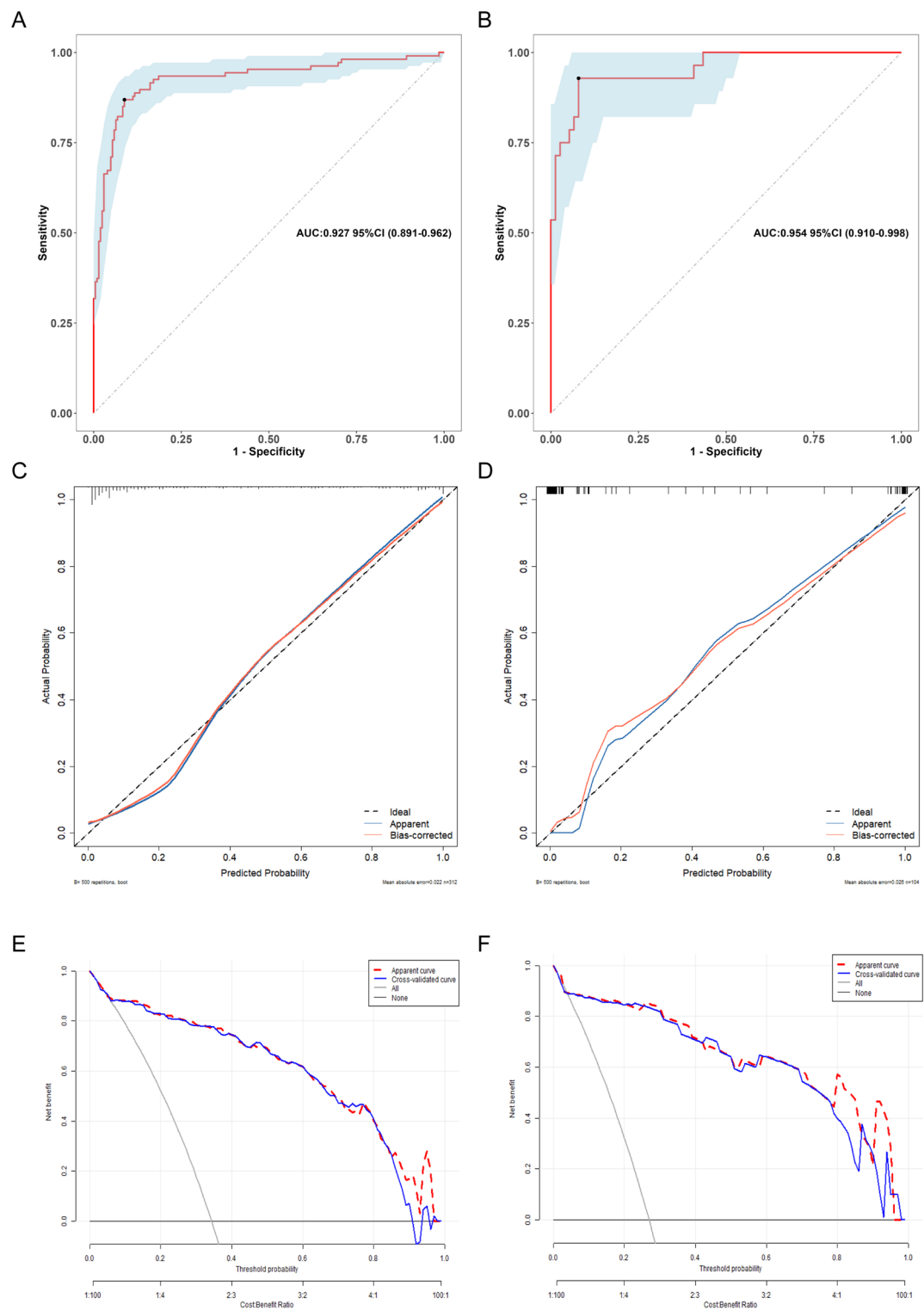
Fig. 5. Evaluation of the prediction model in the training and validation sets. (**A**): The ROC curve of the training set. CI, confidence interval. (**B**): The ROC curve of the validation set. (**C**): The calibration plot of the training set. (**D**): The calibration plot of the validation set. (**E**): The DCA curve of the training set. (**F**): The DCA curve of the validation set.

credibility. Secondly, the TBL for each patient was calculated using a formula, which could be influenced by the volume of perioperative fluids administered. To mitigate this, a uniform fluid regimen was implemented for all participants, with daily fluid intake and output meticulously recorded. Despite these limitations, this study is still a carefully designed prospective cohort study. All enrolled patients underwent consistent blood testing and
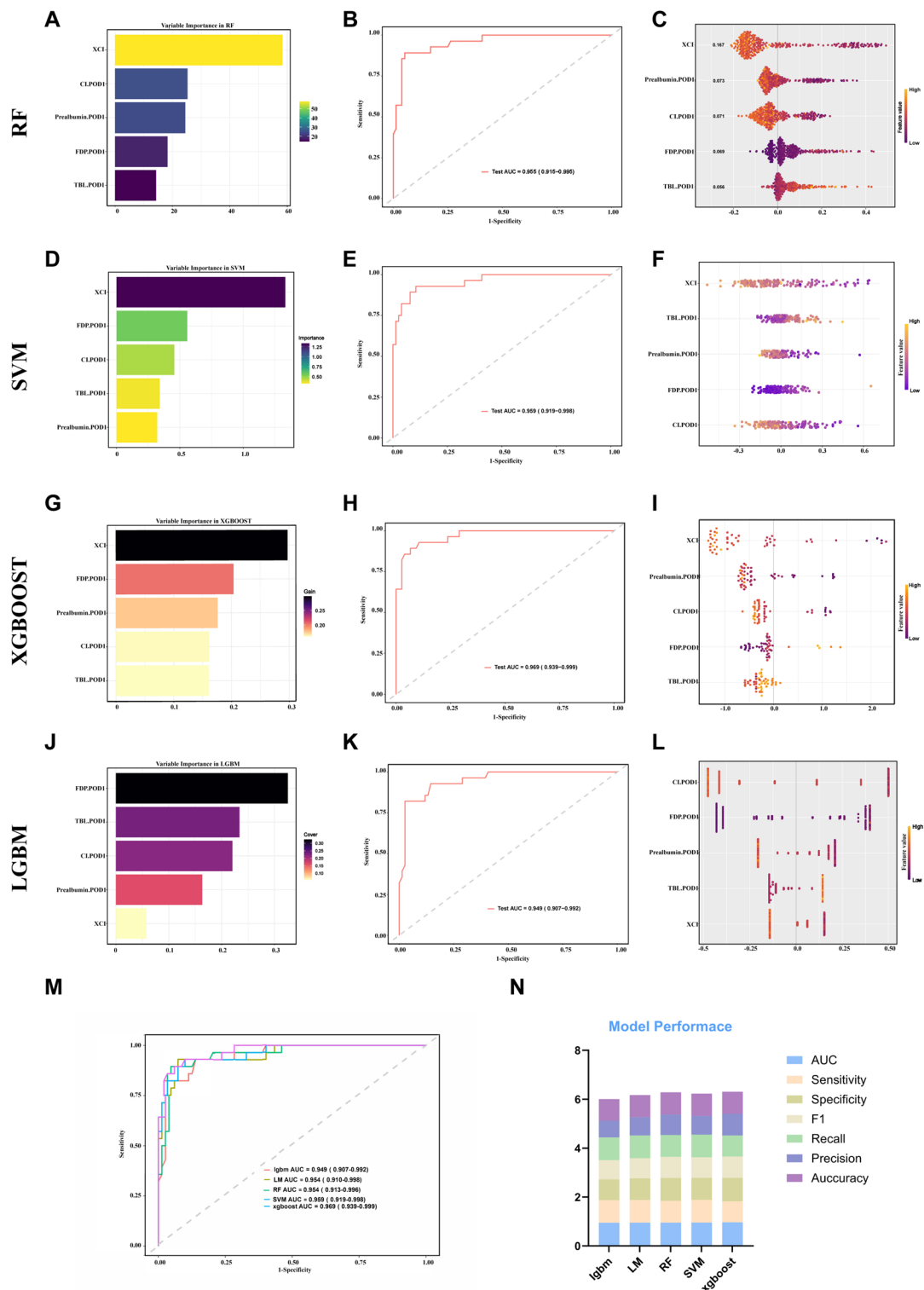
Fig. 6. Validation of the prediction model using multiple machine learning methods. (**A**): Variable importance of the validation set by Random Forest. (**B**): ROC curve of the validation set by Random Forest. (**C**): SHAP diagram of the validation set by Random Forest. (**D**): Variable importance of the validation set by Support Vector Machine. (**E**): ROC curve of the validation set by Support Vector Machine. (**F**): SHAP diagram of the validation set by Support Vector Machine. (**G**): Variable importance of the validation set by Extreme Gradient Boosting. (H): ROC curve of the validation set by Extreme Gradient Boosting. (**I**): SHAP diagram of the validation set by Extreme Gradient Boosting. (**J**): Variable importance of the validation set by Lightgbm. (K): ROC curve of the validation set by Lightgbm. (**L**): SHAP diagram of the validation set by Lightgbm. (**M**): Comparison of ROC curves among various machine learning methods. (**N**): Model performance of the various machine learning methods.

Model	AUC	Sensitivity	Specificity	F1	Recall	Precision	Auccuracy
Lgbm	0.949	0.929	0.842	0.788	0.929	0.684	0.885
LM	0.954	0.929	0.882	0.825	0.929	0.743	0.905
RF	0.954	0.893	0.934	0.862	0.893	0.833	0.914
SVM	0.959	0.929	0.895	0.839	0.929	0.765	0.912
Xgboost	0.969	0.857	0.961	0.873	0.857	0.889	0.901

Table 4. All the ML prediction models' outcomes in the validation set. **Abbreviations**: ML, machine learning. Lgbm, lightgbm. LM, logistic regression model. RF, random forest. SVM, support vector machine. Xgboost, extreme gradient boosting.

related examinations, and were closely monitored for the occurrence of ecchymosis, ensuring the accuracy and reliability of our data.

Conclusion

In the present study, three ML algorithms were employed to screen features, and identified five independent risk factors contributing to ecchymosis: reduced prealbumin, CI and XCI levels, increased FDP, and TBL on POD1. Based on these factors, a predictive model for the occurrence of ecchymosis after TKA was developed and validated using various ML techniques. The implementation of this model in clinical practice may enable a more precise assessment of postoperative bleeding risks and thereby improve blood management and facilitate recovery through early intervention of identified risk factors.

Data availability

Data will be made available from the corresponding author Dr JYL on reasonable request.

References

1. Hutyra, C. A. et al. Patient preferences for surgical treatment of knee osteoarthritis: A Discrete-Choice experiment evaluating total and unicompartmental knee arthroplasty. *J. Bone Joint Surg. Am. Volume*. **102** (23), 2022–2031 (2020).
2. Hamilton, D. F. et al. Reduction in patient outcomes but implant-derived preservation of function following total knee arthroplasty: longitudinal follow-up of a randomized controlled trial. *The Bone & Joint Journal*. **102** (4), 434–441 (2020).
3. Na, A., Middleton, A., Haas, A., Graham, J. E. & Ottenbacher, K. J. Impact of diabetes on 90-Day episodes of care after elective total joint arthroplasty among medicare beneficiaries. *J. Bone Joint Surg. Am. Volume*. **102** (24), 2157–2165 (2020).
4. Liu, D., Dan, M., Martinez Martos, S. & Beller, E. Blood management strategies in total knee arthroplasty. *Knee Surg. Relat. Res.* **28** (3), 179–187 (2016).
5. Arsoy, D., Giori, N. & Woolson, S. Mobile compression reduces Bleeding-related readmissions and wound complications after THA and TKA. *Clin. Orthop. Relat. Res.* **476** (2), 381–387 (2018).
6. Luo, X. et al. Personalized delayed anticoagulation therapy alleviates postoperative bleeding in total knee arthroplasty (TKA) patients. *J. Experimental Orthop.* **11** (4), e70074 (2024).
7. Luo, X. et al. Safety and efficacy of personalised delayed anticoagulation for reducing perioperative blood loss in total knee arthroplasty patients: protocol for a randomised controlled trial. *BMJ open.* **15** (9), e092640 (2025).
8. Yamashita, Y. et al. The association of recurrence and bleeding events with mortality after venous thromboembolism: from the COMMAND VTE registry. *Int. J. Cardiol.* **292**, 198–204 (2019).
9. Verhamme, P. et al. Abelacimab for prevention of venous thromboembolism. *N. Engl. J. Med.* **385** (7), 609–617 (2021).
10. Sidhu, V. S. et al. Effect of aspirin vs Enoxaparin on symptomatic venous thromboembolism in patients undergoing hip or knee arthroplasty: the CRISTAL randomized trial. *Jama* **328** (8), 719–727 (2022).
11. Kleiboer, B. et al. Postoperative bleeding complications in patients with hemophilia undergoing major orthopedic surgery: A prospective multicenter observational study. *J. Thromb. Haemostasis: JTH.* **20** (4), 857–865 (2022).
12. Meng, J. et al. The role of aspirin versus low-molecular-weight heparin for venous thromboembolism prophylaxis after total knee arthroplasty: a meta-analysis of randomized controlled trials. *Int. J. Surg. (London England).* **109** (11), 3648–3655 (2023).
13. Charoencholvanich, K. & Siriwattanasakul, P. Tranexamic acid reduces blood loss and blood transfusion after TKA: a prospective randomized controlled trial. *Clin. Orthop. Relat. Res.* **469** (10), 2874–2880 (2011).
14. Cao, G. et al. Association between preoperative hemoglobin and postoperative moderate and severe anemia among patients undergoing primary total knee arthroplasty: a single-center retrospective study. *J. Orthop. Surg, Res.* **16** (1), 572 (2021).
15. Liu, N. et al. Changes in coagulation functions and hemorheological parameters May predict hematoma formation after total knee arthroplasty. *J. Orthop. Surg, Res.* **11**, 35 (2016).
16. Arsoy, D., Giori, N. J. & Woolson, S. T. Mobile compression reduces Bleeding-related readmissions and wound complications after THA and TKA. *Clin. Orthop. Relat. Res.* **476** (2), 381–387 (2018).
17. Wang, H., Liu, J., Lai, X., Li, X. & Huang, W. The role of Anti-Factor Xa activity in the management of ecchymosis in patients receiving Rivaroxaban after total knee arthroplasty. *Journal Clin. Medicine* **12**(3), 1161 (2023).
18. Wang, J., Zhu, H. L., Shi, Z. J. & Zhang, Y. The application of thromboelastography in Understanding and management of ecchymosis after total knee arthroplasty. *J. Arthroplast.* **33** (12), 3754–3758 (2018).
19. Xiao, L. et al. Risk factors for ecchymosis in patients receiving Rivaroxaban for thromboprophylaxis after total knee arthroplasty: a retrospective cohort study. *J. Clin. Pharm. Ther.* **46** (5), 1281–1287 (2021).
20. Lee, C. R., Kim, C. W., Park, D. H., Kwon, Y. U. & Yoon, J. M. Risk of infection after septic and aseptic revision total knee arthroplasty: A systematic review. *J. Bone Joint Surg. Am. Volume.* **105** (20), 1630–1637 (2023).
21. Larsen, J. B. et al. Exercise and pain neuroscience education for patients with chronic pain after total knee arthroplasty: A randomized clinical trial. *JAMA Netw. open.* **7** (5), e2412179 (2024).
22. Shohat, N., Ludwick, L., Sherman, M. B., Fillingham, Y. & Parvizi, J. Using machine learning to predict venous thromboembolism and major bleeding events following total joint arthroplasty. *Sci. Rep.* **13** (1), 2197 (2023).

23. Sherwood, M. W. et al. Gastrointestinal bleeding in patients with atrial fibrillation treated with Rivaroxaban or warfarin: ROCKET AF trial. *J. Am. Coll. Cardiol.* **66** (21), 2271–2281 (2015).
24. Guijarro, R. et al. Venous thromboembolism and bleeding after total knee and hip arthroplasty. Findings from the Spanish National discharge database. *Thromb. Haemost.* **105** (4), 610–615 (2011).
25. Chen, Y. et al. Changes in thromboelastography to predict ecchymosis after knee arthroplasty: A promising guide for the use of anticoagulants. *Front. Surg.* **9**, 871776 (2022).
26. Dai, J. et al. Artificial intelligence for medicine 2025: navigating the endless frontier. *Innov. Med.* **3** (1), 100120 (2025).
27. Huang, T. et al. Artificial intelligence for medicine: Progress, challenges, and perspectives. *Innov. Med.* **1** (2), 100030 (2023).
28. Shen, Y. et al. Performance analysis of markers for prostate cell typing in single-cell data. *Genes Dis.* **11** (6), 101157 (2024).
29. Greener, J. G., Kandathil, S. M., Moffat, L. & Jones, D. T. A guide to machine learning for biologists. *Nat. Rev. Mol. Cell Biol.* **23** (1), 40–55 (2022).
30. Handelman, G. S. et al. eDoctor: machine learning and the future of medicine. *J. Intern. Med.* **284** (6), 603–619 (2018).
31. Nadler, S. B., Hidalgo, J. H. & Bloch, T. Prediction of blood volume in normal human adults. *Surgery* **51** (2), 224–232 (1962).
32. Gross, J. B. Estimating allowable blood loss: corrected for Dilution. *Anesthesiology* **58** (3), 277–280 (1983).
33. Whiting, D. & DiNardo, J. A. TEG and ROTEM: technology and clinical applications. *Am. J. Hematol.* **89** (2), 228–232 (2014).
34. Ranalli, M. G., Salvati, N., Petrella, L. & Pantalone, F. M-quantile regression shrinkage and selection via the Lasso and elastic net to assess the effect of meteorology and traffic on air quality. *Biometrical J. Biometrische Z.* **65** (8), e2100355 (2023).
35. Zhou, H. et al. Predictive modeling of lower extreme deep vein thrombosis following radical gastrectomy for gastric cancer: based on multiple machine learning methods. *Sci. Rep.* **14** (1), 15711 (2024).
36. Huang, H. & Zhang, J. Prediction of chlorophyll a and risk assessment of water blooms in Poyang Lake based on a machine learning method. *Environmental pollution (Barking, Essex*:) 2024, 347:123501.) 2024, 347:123501. (1987).
37. Nahm, F. S. Receiver operating characteristic curve: overview and practical use for clinicians. *Korean J. Anesthesiology.* **75** (1), 25–36 (2022).
38. Hu, J. & Szymczak, S. A review on longitudinal data analysis with random forest. *Briefings Bioinformatics* **24**(2), 1–11 (2023).
39. Silva, G. F. S., Fagundes, T. P., Teixeira, B. C. & Chiavegatto Filho, A. D. P. Machine learning for hypertension prediction: a systematic review. *Curr. Hypertens. Rep.* **24** (11), 523–533 (2022).
40. Hao, P. Y., Chiang, J. H. & Chen, Y. D. Possibilistic classification by support vector networks. *Neural Networks: Official J. Int. Neural Netw. Soc.* **149**, 40–56 (2022).
41. Hayati Rezvan, P., Lee, K. J. & Simpson, J. A. The rise of multiple imputation: a review of the reporting and implementation of the method in medical research. *BMC Med. Res. Methodol.* **15**, 30 (2015).
42. Bennett, J. A. The consolidated standards of reporting trials (CONSORT): guidelines for reporting randomized trials. *Nurs. Res.* **54** (2), 128–132 (2005).
43. Luo, X. et al. A cross-sectional study unveiling the global impact and future projections through 2060 of osteoarthritis. *European J. public. Health* (2025).
44. Garcia-Casanovas, A. et al. Hospital variation in quality indicators for patient blood management in total knee and hip arthroplasty: a retrospective cohort study. *British journal of anaesthesia* (2024).
45. Dubin, J. A. et al. Trends in deep vein thrombosis prophylaxis after total knee arthroplasty: 2016 to 2021. *J. Arthroplast.* **39** (8S1), S328–S332 (2024).
46. Haft, M. et al. Evaluating the effect of decreasing preoperative hemoglobin on blood Transfusions, major Complications, and periprosthetic joint infection after primary total knee arthroplasty. *The J. Am. Acad. Orthop. Surgeons.* **32** (21), 89–996 (2024).
47. Beyer-Westendorf, J. et al. Rates, management, and outcome of Rivaroxaban bleeding in daily care: results from the Dresden NOAC registry. *Blood* **124** (6), 955–962 (2014).
48. Reel, P. S., Reel, S., Pearson, E., Trucco, E. & Jefferson, E. Using machine learning approaches for multi-omics data analysis: A review. *Biotechnol. Adv.* **49**, 107739 (2021).
49. Shamout, F., Zhu, T. & Clifton, D. A. Machine learning for clinical outcome prediction. *IEEE Rev. Biomed. Eng.* **14**, 116–126 (2021).
50. Heo, K. Y., Rajan, P. V., Khawaja, S., Barber, L. A. & Yoon, S. T. Machine learning approach to predict venous thromboembolism among patients undergoing multi-level spinal posterior instrumented fusion. *J. Spine Surg.* **10** (2), 214–223 (2024).
51. Lin, Z. et al. Utilization of the Caprini risk assessment model(RAM) to predict venous thromboembolism after primary hip and knee arthroplasty: an analysis of the healthcare cost and utilization Project(HCUP). *Thromb. J.* **22** (1), 68 (2024).
52. Jin, J. et al. Development and validation of an ICU-Venous thromboembolism prediction model using machine learning approaches: A multicenter study. *Int. J. Gen. Med.* **17**, 3279–3292 (2024).
53. Ma, S. D. et al. Inherited thrombophilia and portal vein thrombosis in cirrhosis: A systematic review and meta-analysis. *Res. Pract. Thromb. Haemostasis.* **3** (4), 658–667 (2019).
54. Shi, B. et al. Evolutionary warning system for COVID-19 severity: colony predation algorithm enhanced extreme learning machine. *Comput. Biol. Med.* **136**, 104698 (2021).
55. Hoffman, M. & Monroe, D. M. Coagulation 2006: a modern view of hemostasis. *Hematol. Oncol. Clin. N. Am.* **21** (1), 1–11 (2007).
56. Madurska, M. J., Sachse, K. A., Jansen, J. O., Rasmussen, T. E. & Morrison, J. J. Fibrinolysis in trauma: a review. *Eur. J. trauma. Emerg. Surgery: Official Publication Eur. Trauma. Soc.* **44** (1), 35–44 (2018).

Acknowledgements

Author contributions

XFL and WB Contributed equally to this work and conceived the study, WX, JYL and WH designed the study, YY and RXK finished the charts and tables, JYL and XFL drafted the manuscript. All authors approved the final manuscript of this study.

Funding

Declarations

Competing interests
The authors declare no competing interests.

Ethics approval and consent to participate
This study has been approved by the Ethics Committee of The First Affiliated Hospital of Chongqing Medical University (ethical approval No. 2023-079). All eligible patients were fully informed of the benefits and risks associated with the study before signing the informed consent form to participate. All methods were done in accordance with relevant guidelines.

Additional information
Supplementary Information The online version contains supplementary material available at https://doi.org/10.1038/s41598-025-33096-2.

Correspondence and requests for materials should be addressed to W.X., W.H. or J.L.

Reprints and permissions information is available at www.nature.com/reprints.

Publisher's note Springer Nature remains neutral with regard to jurisdictional claims in published maps and institutional affiliations.